Predicting Biomechanical Risk Factors for Division – I Women's Basketball Athletes

Conference Paper · April 2025

DOI: 10.1109/ICASSP49660.2025.10887636

8 authors, including:

Aayushi Vishal Shah
Ahmedabad University
1 PUBLICATION **0** CITATIONS
SEE PROFILE

Harman Jani
Ahmedabad University
1 PUBLICATION **0** CITATIONS
SEE PROFILE

Srishti Sharma
Ahmedabad University
14 PUBLICATIONS **47** CITATIONS
SEE PROFILE

Tolga Kaya
Sacred Heart University
70 PUBLICATIONS **1,121** CITATIONS
SEE PROFILE

ICASSP 2025 - 2025 IEEE International Conference on Acoustics, Speech and Signal Processing (ICASSP) | 979-8-3503-6874-1/25/$31.00 ©2025 IEEE | DOI: 10.1109/ICASSP49660.2025.10887636

Predicting Biomechanical Risk Factors for Division - I Women's Basketball Athletes

Aayushi Shah
Ahmedabad University
Ahmedabad, India
aayushi.s3@ahduni.edu.in

Vanaja Agarwal
Ahmedabad University
Ahmedabad, India
vanaja.a@ahduni.edu.in

Dhairya Shah
Ahmedabad University
Ahmedabad, India
dhairya.s4@ahduni.edu.in

Harman Jani
Ahmedabad University
Ahmedabad, India
harman.j@ahduni.edu.in

Srishti Sharma
Ahmedabad University
Ahmedabad, India
srishti.s1@ahduni.edu.in

Tolga Kaya
Sacred Heart University
Fairfield, USA
kayat@sacredheart.edu

Christopher Taber
Sacred Heart University
Fairfield, USA
taberc@sacredheart.edu

Mehul S. Raval
Ahmedabad University
Ahmedabad, India
mehul.raval@ahduni.edu.in

***Abstract*—Collegiate basketball is characterized by high-impact movements such as jump landings, making athletes more susceptible to injuries. Critical biomechanical factors like knee flexion, lateral trunk flexion, and foot landing asymmetry are strongly associated with injury risk. This study aims to predict six biomechanical risk factors in the landing error scoring system (LESS). The dataset comprises 8600 video frames of counter-movement jumps (CMJs) from 17 NCAA Division I female basketball athletes, recorded from frontal and lateral perspectives and annotated using a customized error annotation algorithm. The study uses the You Only Look Once (YOLOv5nu) model to analyze the basketball athletes' CMJ videos. It demonstrates high reliability in predicting risk factors with an average Box Precision (Box P) of 0.800, recall (R) of 0.877, and mean Average Precision at IoU threshold 0.5 (mAP@0.5) of 0.879.**

***Index Terms*—Biomechanical analysis, collegiate basketball, computer vision, deep learning, injury risk prediction, sports**

I. Introduction

With over 450 million players globally, basketball is a high-impact sport involving frequent jumping, rapid direction changes, and physical contact, all contributing to a high risk of injuries [1], [2]. Biomechanical analysis of jump landings is critical to identifying improper postures and movements that heighten injury risk [3]. The analysis helps coaches and trainers create targeted programs to address these issues and prevent injuries [4].

The Landing Error Scoring System (LESS) [5] evaluates anterior cruciate ligament (ACL) injury risk by assessing jump-landing tasks [3], focusing on critical factors such as knee and hip flexion, trunk flexion, stance width, and foot positioning [6]. Proper knee flexion, stance width, and trunk flexion help absorb impact and reduce stress during landings, minimizing injury risks [7]–[9]. Injury assessment techniques have evolved from traditional methods like optoelectronic systems and force platforms, which are expensive and require specialized training, to modern tools using computer vision (CV) and machine learning (ML) [10], [11]. These technologies enable affordable, real-time analysis of jump-landing tasks using video, detecting movement irregularities instead of manually searching for errors by field experts [12], [13]. Motivated by the above studies, the proposed approach uses video analysis to predict biomechanical risk factors for LESS. The paper's contributions are: i. Creating a CMJ video dataset and developing a customized error annotation algorithm. ii. Developing and analyzing a baseline model using You Only Look Once (YOLO) [14] for video analysis.

II. Methods

A. Participants

This study was approved by the Sacred Heart University Institutional Review Board, approval number 170720A, on 9/14/2020. We recruited 17 participants from the Division-I Women's Basketball team with 20 videos from the 2022-23 season and 23 videos from the 2021-22 season, with a mean age of 21.00 (±3.00) years, mean height of 174.21 (±19.27) cm, and mean body mass of 73.98 (±11.52) kg. The data included 43 trials, with over 8600 video frames from the frontal and lateral planes.

B. Data Acquisition

Two Panasonic LUMIX FZ80 4K digital cameras featuring 18.1-megapixel sensors and 60x zoom DC VARIO lenses (20-1200mm focal range, F2.8-5.9 aperture) were positioned 136 inches from the jump spot to capture high-resolution, stabilized videos from frontal and lateral angles. Athletes performed CMJs on dual force plates (FDlite, Vald Performance, Brisbane, QL, AUS) with a 1000 Hz sampling rate as part of their regular training. CMJ sessions, held during the week's first practice, involved a standardized warm-up followed by jumps aimed at achieving maximum height with minimal ground contact time. Each session included three CMJs, with the best jump of the series from these jumps being analyzed.

C. Video Processing

Fig. 1 visualizes the workflow in which frames are extracted from the video footage and the MediaPipe Pose (MPP) [15]

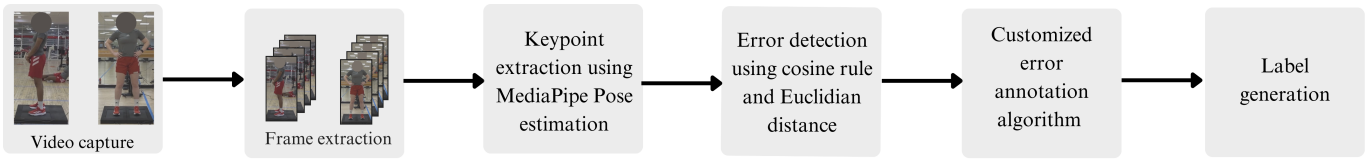

Fig. 1: The flow for video processing and label generation for frontal and lateral planes.

library is employed to extract 2D coordinates of biomechanical key points for movement analysis. These coordinates help categorize errors in executing the CMJ performed by athletes, with labels automatically generated in YOLO format for the model training by a customized error annotation algorithm 1.

D. Frame Extraction

The videos in this study were initially recorded at a resolution of 1920×1080 pixels. All videos were resized to 640×640 pixels to ensure compatibility with the YOLO model used in the study. Furthermore, to standardize the dataset, each video was uniformly segmented into 200 frames, and the frame rate *(fps)* was calculated using the formula $fps = 200/(\textit{length of the video in seconds})$. Additionally, all the videos were rotated to correct the camera tilt, ensuring the force plate was parallel to the ground to be consistent with the error thresholds provided by the expert.

E. Keypoint Extraction

The MPP framework [15] utilizes a two-stage model pipeline based on a MobileNetV2-like CNN and enhanced by the BlazePose variation [16], which was used to extract key points from the human body. While MPP extracts 33 key points from the human body, this study focused on 12 key points (11, 12, and 23 to 32) related to high-risk movements and postures of the lower extremities during jump landings, as depicted in Fig. 2.

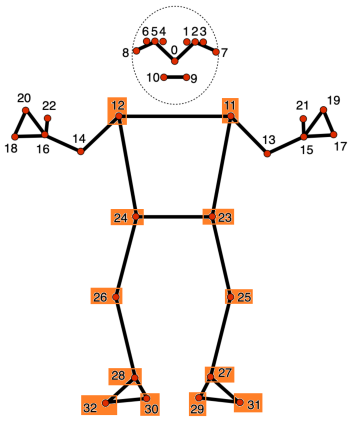

Fig. 2: Definition of body key points in MPP [15] The highlighted key points are used in the proposed work.

F. Computation of Biomechanical Features

LESS [5] comprises 17 biomechanical features; however, we have selected and analyzed six (three from the frontal plane and three from the lateral plane) as they directly indicate biomechanical instability during jump landings [3].

1) Lateral Trunk Flexion: We calculate the degree of lateral deviation from the frontal viewpoint using the vector dot product. Here, one vector connects the hip midpoint, refer to (23, 24) in Fig. 2, to the top of the frame, and the other connects the hip midpoint to the shoulder midpoint (11, 12) [3].

2) Stance Width: We calculate stance width by dividing the Euclidean distance between shoulder key points (11, 12) by the distance between the ankle key points (27, 28) [3].

3) Foot Landing Symmetry: We compare the y-coordinates of the right foot index (32) and the left foot index (31) to assess foot landing symmetry [3].

4) Knee Flexion: Due to the positioning of the camera, the left knee occluded the right knee, making it impossible to compute the right knee's flexion angle accurately. To assess the left knee flexion from a lateral perspective, we calculate the left (23, 25, 27) knee flexion angle using the vector dot product [3].

5) Trunk Flexion: To assess left trunk flexion, we compute the angle created by the key points at the left shoulder (11), hip (23), and knee (25) using the vector dot product [3]. Moreover, hip flexion and trunk flexion are complementary motions, and an error in trunk flexion also indicates an error in hip flexion.

6) Ankle Plantar Flexion: The y-coordinate of the heel (29, 30) and of the foot index (31, 32) are compared to assess ankle plantar flexion [3].

Table I outlines the injury risk error thresholds. A feature is considered to indicate an error only if its computed value meets the requirement of the error threshold.

TABLE I: The injury risk errors as used in LESS [5].

Biomechanical Feature	**Calculation**	**Error threshold**
Stance Width	Ratio of Euclidean distances	Ratio $<$ 0.8 (narrow stance), Ratio $>$ 1.2 (wide stance)
Lateral Trunk Flexion	Angle between imaginary lines using cosine formula	Right lateral flexion if Angle $>$ 0°, else left lateral flexion.
Foot Landing Symmetry	Absolute difference in y-coordinates	Difference $>$ 5 units
Knee Flexion	Cosine of three-point coordinates	Knee flexion angle $<$ 30°
Trunk Flexion	Cosine of three-point coordinates	Trunk flexion angle between -4° and 4°
Ankle Plantar Flexion	Comparison of y-coordinates	Heel y-coordinate $<$ Foot index y-coordinate

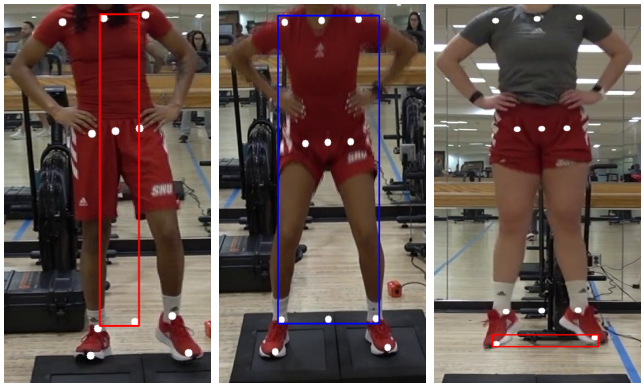

(i) (ii) (ii)

Fig. 3: Errors in biomechanical features from the frontal plane: i. Right lateral flexion, ii. Narrow stance, iii. Foot asymmetry.

(i) (ii) (ii)

Fig. 4: Errors in biomechanical features from the lateral plane: i. Knee flexion, ii. No trunk flexion, iii. Ankle plantar flexion.

G. Coordinates and Normalization

The coordinates obtained from the key points of the MPP library are in pixel values, representing their exact locations on the image. These coordinates define error locations and help to draw tight bounding boxes. To ensure consistency and accurate predictions across different images, normalization is applied by converting pixel values to relative values by dividing them by the image dimensions. This process generates normalized centre coordinates and dimensions of the bounding boxes [17]. It allows the model to be more robust and generalized across datasets with images of different sizes.

H. Video Annotation

We encountered difficulties using manual video annotation tools like Kinovea [18] and Roboflow [19] to create bounding boxes for our dataset. Drawing the tightest bounding boxes was highly time-consuming and prone to errors. We developed a customized error annotation algorithm 1 to address these limitations that automates image annotation by leveraging the MPP estimation library [15]. This algorithm identifies four extreme coordinates from the keypoint set to define a bounding box. In this algorithm, the pixel coordinate system assumes the origin at the top-left corner of the image, with the y-coordinate increasing downward, and the x-coordinate increasing rightward. These coordinates are then normalized and stored in the YOLO format [17].

For knee flexion, we employed a semantic segmentation tool provided by Roboflow [19], designating the lower half of the athlete's body as the foreground and the rest as the background. This approach ensured that the model focused on the athlete's lower body for biomechanical analysis. Figures 3 and 4 illustrate the various injury-risk errors annotated on video frames.

I. Model Training

We use YOLO because of its high efficiency, speed, and ability to predict multiple bounding boxes and class probabilities simultaneously [14], [20]. The model was pre-trained on the COCO dataset [21] and further developed using transfer learning on our custom train dataset. Before training the model, we split the data into 70:20:10 ratio as train, validation, and test sets. Once the model was trained, we tested the model on the test dataset using precision (mAP@0.5), box P and recall (R). For the model training, we utilized an NVIDIA Quadro P5000 GPU, equipped with CUDA version 12.5, Driver version 555.42.06, 16 GB GDDR5 memory, with a power usage of 42W - 180W, and operating at a temperature of 38°C.

Algorithm 1 Error Annotation Algorithm

Input: Frontal and lateral video frames.
Output: Normalized bounding box coordinates.

I. Extract X and Y co-ordinate of required keypoints

$(x_1, y_1) \leftarrow$ Top-Left Keypoint
$(x_2, y_2) \leftarrow$ Top-Right Keypoint
$(x_3, y_3) \leftarrow$ Bottom-Left Keypoint
$(x_4, y_4) \leftarrow$ Bottom-Right Keypoint

II. Calculate Bounding Box Coordinates

Top-Left X-Coordinate $\leftarrow min(x_1, x_3)$
Top-Left Y-Coordinate $\leftarrow min(y_1, y_2)$
Bottom-Right X-Coordinate $\leftarrow max(x_2, x_4)$
Bottom-Right Y-Coordinate $\leftarrow max(y_3, y_4)$

III. Labeling of the bounding box

Assign a label ID to the bounding box based on error conditions related to key point positions, as Table I outlines.

IV. Normalization of the coordinates

Normalize and save the bounding box coordinates to YOLO format as (class, x_{center}, y_{center}, width, height).

III. Results And Discussion

A. Statistical Analysis of Dataset

Studying variability in the dataset is crucial as it underscores the need for individualized training to reduce injury risk and enhance performance. Table II summarizes the dataset's statistical properties.

TABLE II: Biomechanical feature statistics from the dataset.

Biomechanical Feature	Median	Range	Standard Deviation
Stance Width	1.044	[0.072, 2.266]	00.135
Lateral Trunk Flexion	-0.561	[-18.434, 13.851]	02.202
Foot Landing Symmetry	5.000	[0.000, 177.000]	08.710
Knee Flexion	8.253	[0.001, 102.722]	21.753
Trunk Flexion	3.699	[-73.607, 114.225]	24.534
Ankle Plantar Flexion	5.000	[0, 40]	05.512

It indicates that the stance width remained constant, within a narrow range and low standard deviation, which suggests a normal stance in most videos. Lateral trunk flexion showed a slight leftward deviation with moderate variation. Foot landing symmetry displayed notable asymmetries reflected in its extensive range and moderate standard deviation. Knee and trunk flexion displayed wide variation during the CMJ, with high standard deviation and extensive range. In contrast, ankle plantar flexion showed relatively consistent movement, with a narrower range and low standard deviation.

B. Parameter Tuning

To optimize the hyperparameters of the YOLOv5nu model, we employed an inbuilt genetic algorithm [22], resulting in a batch size of 16, learning rates of 0.01, momentum of 0.937, weight decay of 0.0005, and warm-up momentum of 0.8. The model was trained for 300 epochs. We used stochastic gradient descent for biomechanical error detection with a learning rate of 0.01 and momentum of 0.9. In contrast, AdamW was used for knee flexion optimization with a learning rate of 0.001667 and a momentum of 0.9.

C. Object Detection and Ablative Study

Object detection was utilized for five of six biomechanical features, while semantic segmentation was explicitly applied to knee flexion. This choice reduced noise by focusing on the athlete's lower half, enabling more precise identification of key joint regions. To ensure accurate performance metrics, we used a weighted average that accounts for the significance of each error type. This was done by multiplying the number of instances for each label by its performance metric and dividing the obtained result by the total number of frames. Table III presents the weighted average performance metrics for the YOLOv5nu object detection and segmentation models. The results indicate effective detection of stance width, lateral trunk flexion, knee flexion, and trunk flexion. However, the model exhibited moderate performance for foot landing symmetry and comparatively poor performance for ankle plantar flexion due to occlusion of the right leg by the left leg in the lateral video frames.

Additionally, we tested alternative models, such as Mask R-CNN and Darknet, but found that YOLO variants consistently outperformed them. Therefore, we conducted a detailed comparison of YOLO variants. We incorporated both lateral and frontal views to predict risk factors where the bounding boxes in the frames represent the predicted risk factors.

TABLE III: Weighted average performance metrics for YOLOv5nu.

Error Type	Box P	R	mAP@0.5
Stance Width	0.896	0.976	0.973
Lateral Trunk Flexion	0.792	0.930	0.924
Foot Landing Symmetry	0.677	0.839	0.815
Knee Flexion	0.961	0.979	0.983
Trunk Flexion	0.831	0.939	0.941
Ankle Plantar Flexion	0.648	0.603	0.641
Average	0.800	0.877	0.879

We ruled out a multi-view approach due to high costs and resource demands [11]. The poor results for ankle plantar flexion stem from this limitation, but our framework works well with datasets that avoid lower-body occlusion [23]. Table IV shows the performance of YOLOv5nu against the other variants of YOLO [24]. YOLOv8n was selected for its advanced architecture and higher precision, YOLOv10n for its experimental enhancements, and YOLOv3 Tiny for its lightweight design, and real-time speed. Table IV results underscore YOLOv5nu's robustness and reliability, making it the most effective model in this study.

TABLE IV: Percentage improvement in YOLOV5nu compared to other variants (weighted average across all errors).

Metric	YOLOv5nu vs. YOLOv8n(%)	YOLOv5nu vs. YOLOv10n(%)	YOLOv5nu vs. YOLOv3Tiny(%)
Box P	-0.311	11.355	1.881
R	0.468	48.699	6.456
mAP@0.5	0.139	53.521	5.296

IV. Conclusion

Lower extremity injuries can significantly affect athletes' performance and careers. Our proposed approach demonstrates strong predictive capabilities for identifying risk factors, achieving high precision, recall, and mAP@0.5. However, data imbalance and occlusion limit the model's performance. To address these issues, we plan to expand the dataset and explore multi-view camera setups in future work. Additionally, we aim to deploy the model on mobile applications to facilitate real-time analysis, making it more accessible for athletic training and injury prevention. While privacy concerns prevent us from publicly sharing the dataset used in this study, which involves athletes from Sacred Heart University, similar public datasets are available. Our framework can be readily applied to these datasets to achieve comparable results [23].

V. Acknowledgement

The research team wants to thank the players and coaching staff at Sacred Heart University for their cooperation and support. They are also grateful for Sacred Heart University, USA, and Ahmedabad University, India's support for providing the research platform.

REFERENCES

[1] J. Taborri, L. Molinaro, A. Santospagnuolo, M. Vetrano, M. C. Vulpiani, and S. Rossi, "A machine-learning approach to measure the anterior cruciate ligament injury risk in female basketball players," *Sensors*, vol. 21, no. 9, p. 3141, 2021.

[2] J. B. Taylor, K. R. Ford, A.-D. Nguyen, L. N. Terry, and E. J. Hegedus, "Prevention of lower extremity injuries in basketball: a systematic review and meta-analysis," *Sports health*, vol. 7, no. 5, pp. 392–398, 2015.

[3] S. Sharma, S. Divakaran, T. Kaya, C. Taber, and M. S. Raval, "A framework for biomechanical analysis of jump landings for injury risk assessment," in *2023 IEEE 28th Pacific Rim International Symposium on Dependable Computing (PRDC)*, pp. 327–331, IEEE, 2023.

[4] S. Norouzi, F. Esfandiarpour, S. Mehdizadeh, N. K. Yousefzadeh, and M. Parnianpour, "Lower extremity kinematic analysis in male athletes with unilateral anterior cruciate reconstruction in a jump-landing task and its association with return to sport criteria," *BMC musculoskeletal disorders*, vol. 20, pp. 1–9, 2019.

[5] D. A. Padua, S. W. Marshall, M. C. Boling, C. A. Thigpen, W. E. Garrett Jr, and A. I. Beutler, "The landing error scoring system (less) is a valid and reliable clinical assessment tool of jump-landing biomechanics: the jump-acl study," *The American journal of sports medicine*, vol. 37, no. 10, pp. 1996–2002, 2009.

[6] D. A. Padua, L. J. DiStefano, A. I. Beutler, S. J. De La Motte, M. J. DiStefano, and S. W. Marshall, "The landing error scoring system as a screening tool for an anterior cruciate ligament injury–prevention program in elite-youth soccer athletes," *Journal of athletic training*, vol. 50, no. 6, pp. 589–595, 2015.

[7] L. Guo, J. Zhang, Y. Wu, and L. Li, "Prediction of the risk factors of knee injury during drop-jump landing with core-related measurements in amature basketball players," *Frontiers in Bioengineering and Biotechnology*, vol. 9, p. 738311, 2021.

[8] M. C. Stuelcken, D. B. Mellifont, A. D. Gorman, and M. G. Sayers, "Mechanisms of anterior cruciate ligament injuries in elite women's netball: a systematic video analysis," *Journal of sports sciences*, vol. 34, no. 16, pp. 1516–1522, 2016.

[9] L. J. DiStefano, S. W. Marshall, D. A. Padua, K. Y. Peck, A. I. Beutler, S. J. de la Motte, B. S. Frank, J. C. Martinez, and K. L. Cameron, "The effects of an injury prevention program on landing biomechanics over time," *The American journal of sports medicine*, vol. 44, no. 3, pp. 767–776, 2016.

[10] A. Ferrer, R. Twycross-Lewis, and N. Maffulli, "Anterior cruciate ligament deficiency: rotational instability in the transverse plane. a preliminary laboratory in vivo study.," *Muscles, Ligaments & Tendons Journal (MLTJ)*, vol. 9, no. 1, 2019.

[11] T. Neri, R. Testa, L. Laurendon, M. Dehon, S. Putnis, S. Grasso, D. A. Parker, F. Farizon, and R. Philippot, "Determining the change in length of the anterolateral ligament during knee motion: a three-dimensional optoelectronic analysis," *Clinical Biomechanics*, vol. 62, pp. 86–92, 2019.

[12] F. Della Villa, M. Buckthorpe, A. Grassi, A. Nabiuzzi, F. Tosarelli, S. Zaffagnini, and S. Della Villa, "Systematic video analysis of acl injuries in professional male football (soccer): injury mechanisms, situational patterns and biomechanics study on 134 consecutive cases," *British journal of sports medicine*, vol. 54, no. 23, pp. 1423–1432, 2020.

[13] C. Roygaga, D. Patil, M. Boyle, W. Pickard, R. Reiser, A. Bharati, and N. Blanchard, "Ape-v: Athlete performance evaluation using video," in *Proceedings of the IEEE/CVF Winter Conference on Applications of Computer Vision*, pp. 691–700, 2022.

[14] J. Redmon, S. Divvala, R. Girshick, and A. Farhadi, "You only look once: Unified, real-time object detection," in *Proceedings of the IEEE conference on computer vision and pattern recognition*, pp. 779–788, 2016.

[15] Mediapipe, "Pose." https://chuoling.github.io/mediapipe/solutions/pose.html. [Accessed 07-09-2024].

[16] G. for Developers, "Pose landmark detection guide — google ai edge." https://ai.google.dev/edge/mediapipe/solutions/vision/pose_landmarker. [Accessed 07-09-2024].

[17] "YOLOv8 Label Format: A Step-by-Step Guide - YOLOv8." https://yolov8.org/yolov8-label-format/#google_vignette. [Accessed 07-09-2024].

[18] J. Charmant, "Kinovea." https://www.kinovea.org/. [Accessed 07-09-2024].

[19] "Roboflow: Computer vision tools for developers and enterprises." https://roboflow.com/. [Accessed 07-09-2024].

[20] S.-D. Achirei, M.-C. Heghea, R.-G. Lupu, and V.-I. Manta, "Human activity recognition for assisted living based on scene understanding," *Applied Sciences*, vol. 12, no. 21, p. 10743, 2022.

[21] T.-Y. Lin, M. Maire, S. Belongie, J. Hays, P. Perona, D. Ramanan, P. Dollár, and C. L. Zitnick, "Microsoft coco: Common objects in context," in *Computer Vision–ECCV 2014: 13th European Conference, Zurich, Switzerland, September 6-12, 2014, Proceedings, Part V 13*, pp. 740–755, Springer, 2014.

[22] Ultralytics, "Hyperparameter Tuning — docs.ultralytics.com." https://docs.ultralytics.com/guides/hyperparameter-tuning/#preparing-for-hyperparameter-tuning. [Accessed 10-09-2024].

[23] N. Blanchard, K. Skinner, A. Kemp, W. Scheirer, and P. Flynn, "" keep me in, coach!": A computer vision perspective on assessing acl injury risk in female athletes," in *2019 IEEE Winter conference on applications of computer vision (WACV)*, pp. 1366–1374, IEEE, 2019.

[24] Ultralytics, "Models Supported by Ultralytics — docs.ultralytics.com." https://docs.ultralytics.com/models/#featured-models. [Accessed 12-09-2024].